

Tropospheric Variation of Point Refractivity Gradient and Geoclimatic Factor over a Coastal Location in Tropical Nigeria

Okikiade Adewale Layioye*

Abstract

Accurate assessment of refractivity gradient and geoclimatic factor is crucial for maintaining reliable radio signal propagation in clear-air environments. These parameters are essential for determining the fade margin necessary to ensure a stable and effective wireless radio link, given the unstable nature of the atmosphere through which the signals travel. It is crucial to have accurate knowledge of these characteristics, particularly at microwave antenna heights of around 70 m, in order to sustain a functional line-of-sight link even in the most adverse weather circumstances. The lack of adequate studies on this topic for Lagos made the investigation necessary. This study utilized meteorological data, including surface air temperature, dew point temperature, and relative humidity, obtained from the European Centre for Medium-Range Weather Forecasts archive over a period of 6 years. The point refractivity gradient at 70 m and refractive conditions were estimated for Ikeja, Lagos State, which is a coastal city within tropical Nigeria. The study's findings demonstrate that the geoclimatic factor and point refractivity gradient in the studied area change with the seasons. Specifically, for Ikeja and its environs, the research found that the average point refractivity gradient and geoclimatic factor at 70 m above ground level are -196.30 N-units/km and $1.06E - 04$, respectively. These findings indicate that radio waves propagating in this region at the specified altitude are likely to experience super refraction under both rainy and clear-air atmospheric conditions. In addition, wet months show high variability of refractivity gradient of about -167.828 N-units/km due to increase in the water vapor in the atmosphere compared to the dry periods with low variability of about -196.296 N-units/km. Also, the average values of the geoclimatic factor in the wet season are $8.66774E - 05$ and that of the dry season is 0.000133 . This suggests that extremely poor radio propagation condition is expected to take place within the dry months, especially in November. This study highlights the significant influence of meteorological parameters such as temperature, pressure, and humidity on the quality of services provided by inter-terrestrial radio communication links, including GSM networks, wide area networks, and radio and TV broadcasts. The insights gained from this research are particularly valuable for radio engineers involved in the design and configuration of inter-terrestrial microwave links in Ikeja and its environs, facilitating optimal quality of service even during adverse weather conditions.

*Author for Correspondence

Okikiade Adewale Layioye
E-mail: oalayioye@futa.edu.ng

Student, Department of Physics, Federal University of Technology, Akure, Nigeria

Received Date: June 10, 2024
Accepted Date: July 07, 2024
Published Date: July 10, 2024

Citation: Okikiade Adewale Layioye. Tropospheric Variation of Point Refractivity Gradient and Geoclimatic Factor over a Coastal Location in Tropical Nigeria. Journal of Remote Sensing & GIS. 2024; 15(2): 28–42p.

Keywords: GSM Networks, WAN, Geoclimatic factor, radio frequency, signal transmission, microwave antenna

INTRODUCTION

Due to the growing demand for better radio wave propagation technologies, the idea of wireless communication in the lower atmospheric layer has recently been critical to radio communications. The sophistication and ever-changing trend of radio communication has resulted in its widespread

applicability. However, given the high demand and widespread use of wireless communications, there is a need to investigate the features that lead to signal fading during transmission [1–3].

The propagation of electromagnetic waves is greatly influenced by the Earth's atmosphere, and this is important for radio communication and radar systems. Since it is a dynamic medium, changes in parameters like temperature, pressure, and humidity impact the characteristics of the atmosphere. The tropospheric refractive index is affected by these fluctuations, and it is essential to clear air propagation processes. Considering signal transmission under clear air conditions, particularly on terrestrial line-of-sight links, many atmospheric processes cause signal losses on the transmission link [4–6]. As a result, this diminishes radio wave propagation and radar performance by causing phenomena including multipath fading, interference, and attenuation to impact radio signals [5, 7]. Clear-air fading caused by severe refractive layers in the environment comprises beam spreading, antenna decoupling, surface multipath, and atmospheric multipath [8]. Multipath fading is one of the most common fading phenomena in tropospheric transmission, as demonstrated via terrestrial line of sight links [7, 9].

When developing a dependable radio communication network, it is important to account for signal fades or changes [5]. Many authors have offered numerous solutions to address the issue of radio propagation in various parts of the world. These strategies were developed using radio propagation data from the regions in question [3, 8, 10]. These scholars have suggested that the geoclimatic factor is a very significant variable for representing the geographical and climatic characteristics of the area studied [3]. Thus, the geoclimatic factor is one of the variables taken into account while determining the multipath fade depth at any given time in a radio communication link [11, 12]. The temperature, pressure, relative humidity, and water vapor pressure are the main parameters that are used to determine the geoclimatic factor. A radio refractive index called n is utilized to describe the impact of climatic conditions [3, 13, 14]. The refractivity gradient, which is a function of radio refractivity and height above ground, can also be used to determine the multipath fading at any given time in a radio link, and it is therefore related to the radio refractive index [5].

To design the communication link, the ITU-R (International Telecommunications Union – Radiocommunication Sector) advises using the following parameters: the atmospheric radio-refractive index, the refractivity gradient, the point refractivity gradient, and the geoclimatic factor. This will allow for the variation of the atmospheric state as the values of the meteorological parameters change [11, 15]. Anomalous propagation is a result of irregular atmospheric conditions, refocusing rays of radio signals either upwards or downwards, leading to sub-refraction (when it gets directed upwards) or super-refraction and ducting (when it is forced downwards) [16]. Due to this erraticism, a comprehensive study of the anomalous characteristics of radio wave transmission over coastal tropical areas is essential, so as to provide a better enhancement to the strength of radar and radio communication systems. Since the communication link must be at an optimal performance, then the transmission system must be carefully planned [2, 5, 17]. This can only be achieved by proper evaluation of radio refractivity, point refractivity gradient and the geoclimatic factor for the location under study.

Currently, several research works on radio refractivity have been carried out for different regions within tropical regions, however this work covers a coastal area within a tropical climate. Bettouche et al. [1] computed the geoclimatic factor and point refractivity for Quebec-Canada. The research work presented by Odedina and Afullo [3] showed the use of spatial interpolation technique to determine geoclimatic factor and fade depth calculation for Southern Africa. Ojo et al. [8] estimated the clear-air fade depth due to radio climatological variables for the applications of microwave link in Akure, Nigeria. Etokebe et al. [11] used the inverse distance weighting spatial interpolation technique to acquire missing data at different heights, and then reported the seasonal variation of refractivity gradient and geoclimatic factor. Oluwafemi and Olla [12] used meteorological data to determine the geoclimatic factor for Nigeria.

In this research work, the main goal is to use meteorological data for Ikeja collected from the European Centre for Medium-Range Weather Forecasts (ECMWF) database to calculate the point refractivity gradient and geoclimatic factor accordingly, over the first 70 m above ground level. Also, this will be accompanied by a cumulative distribution of the geoclimatic factor over Ikeja. Ikeja is a mega city situated in the South-West region of Nigeria. The other sections of this paper are organized as follows: The second section provides a theoretical background and overview of the geoclimatic factor. The third section discusses the methodology and data collection. The penultimate section presents the study's findings, and the final section concludes the paper.

THEORETICAL BACKGROUND

Overview of the Geoclimatic Factor

The geoclimatic factor (K) is a variable that may be obtained by first determining other propagation factors such as refractivity and refractivity gradient [16]. The ITU-R suggests the following expressions [16, 17], to calculate radio refractivity and its gradient. The radio refractivity can be determined using [16, 17]:

$$N = (n - 1) \times 10^{-6} \quad (1)$$

where N is the radio refractivity in N-units and n is the refractive index, expressed by [16, 17]:

$$N = \frac{77.6}{T} (P + 4810 \frac{e}{T}) \quad (2)$$

The dry and wet refractivity are both included in this statement. T is the absolute temperature in Kelvin, P is the total atmospheric pressure in hectopascals (hPa), and e is the partial water vapor pressure in hPa. The partial water vapor pressure is calculated as follows using the relative humidity (RH) of the air in percentage [16, 17]:

$$e = \frac{RH \cdot e_s}{100} \quad (3)$$

The saturated water vapor pressure, denoted as e_s , can be found using the following formula [16, 17]:

$$e_s = 6.1121 \exp\left(\frac{17.502t}{t+240.97}\right) \quad (4)$$

where t is the temperature in degrees Celsius ($^{\circ}\text{C}$). The formula for the long-term mean dependence of the refractive index n on height h is as follows [16, 17]:

$$n(h) = 1 + N_0 \cdot 10^{-6} \exp\left(\frac{-h}{h_0}\right) \quad (5)$$

where h_0 is the scale height in kilometers and N_0 is the average atmospheric refractivity extrapolated to sea level.

For terrestrial pathways, statistically it is noted that $N_0 = 315$ and $h_0 = 7.35$ km. With h_s representing the height of the Earth's surface above sea level in kilometers, we can use this to calculate the surface refractivity N_s at the earth's surface from N_0 as follows [16, 17]:

$$N_s = N_0 \exp\left(\frac{h_s}{h_0}\right) \quad (6)$$

The formula that gives the radio refractivity gradient (N_G) in N-units/km is [16, 17]:

$$N_G = \frac{N_1 - N_2}{h_1 - h_2} \quad (7)$$

where N_1 and N_2 are the radio refractivity values at heights h_1 and h_2 , respectively. Several works describe the process for determining the geoclimatic factor (K). The following formula may be used to estimate K for quick planning in a highly fair and precise manner [16]:

$$K = 10^{-4.6-0.0027dN_1} \quad (8)$$

where dN_1 is the point refractivity gradient in the lowest 65 m of the atmosphere, not exceeded for 1% of an average year.

The point refractivity gradient may be approximated using the formula [16]:

$$dN_1 = \frac{dN}{dh} \Big|_{h \leq 65 \text{ m}} \quad (9)$$

The values dN_1 can be obtained at the h_1 nearest to 65 m, where $60 \text{ m} < h_1 < 70 \text{ m}$. The evaluation of the geoclimatic factor in different regions is based on these formulas and methods.

Refractive Conditions

The positive N_G values signify that there will be sub-refraction, which results in loss due to diffraction, while negative values of beyond -100 N-units/km leads to bending of the radio signals towards the Earth. However, for a normal refraction, the gradient should be -40 N-units/km, else the conditions in Table 1 will be dominant [18–20]. Therefore, the different refractive conditions that can be estimated through the determination of the refractivity gradient are presented in Table 1.

METHODOLOGY

Study Location

This work estimates the point refractivity gradient and geoclimatic factor for radio wave propagation via the troposphere in Ikeja and its surrounding land and islands. This study site is a coastal location in Nigeria. Since Nigeria has a tropical climate, then Ikeja can be classified under tropical coastal climate. The geographic coordinates of Ikeja are 3.3515° E longitude and 6.6018° N latitude. It has two seasons which are the rainy and dry seasons. Based on the statistical analysis performed on the rainfall data for Lagos State, over the period under study in this work, it was observed that mid-March through September is the wet season and October through early-March is the dry season for this coastal location, and this agrees with earlier studies [21, 22]. The physical location of Ikeja, Lagos State can be viewed in Figure 1.

Data Collection and Computational Analysis

The 6-year data (2018–2023) used in this work was extracted from the database of the ECMWF database. The synoptic records with resolution of $0.75^\circ \times 0.75^\circ$, for temperature (K), pressure (hPa) and dew point temperature (K) at the surface level were obtained, and thus surface RH (%) was calculated. The necessary data at 70 m altitude was obtained from synoptic records at different model levels, also obtained from the ECMWF database.

Equation (3) was used to obtain the water vapor pressure e (hPa) from the RH (%) values. Equation (2) was utilized to calculate N_s and N_h at 70 m altitude. Equation (9) was used to calculate the dN_1 values at height of 70 m. In addition, Equation (8) was used to determine the K values. Consequently, the monthly and diurnal averages were computed for N_s , dN_1 , and K , and then comparisons were made. Lastly, the long-term cumulative distribution function (CDF) was performed on the obtained dN_1 values.

Table 1. Refractive conditions and their corresponding refractivity gradients [18–20].

Refractive condition	Refractivity gradient (N-units/km)
Sub-refractive	> -40
Super-refractive	$-157 < N_G < -40$
Ducting	< -157



Figure 1. Map of Nigeria showing the study location marked in red.

RESULTS AND DISCUSSION

Monthly and Diurnal Variation of Radio Refractivity

The monthly average refractivity statistics for Ikeja are presented in Table 2 and Figure 2. Table 2 illustrates that the average surface refractivity varies throughout the year, with peak values occurring between March and October across all the years considered. It was also notably observed from Figure 2 that surface refractivity follows a similar trend across all the years, and it seems to be highest in the rainy season and lowest in the dry season.

Table 2. Monthly average values of surface refractivity.

Month	Radio Refractivity, N-units						
	2018	2019	2020	2021	2022	2023	2018–2023
Jan	367.923	379.136	356.364	382.313	365.412	373.246	370.732
Feb	385.446	386.915	369.084	380.786	380.481	377.888	380.035
Mar	389.006	392.349	388.916	388.211	389.724	385.118	389.221
Apr	390.214	393.879	387.120	388.362	387.522	388.255	389.225
May	388.446	391.710	391.308	387.512	390.306	392.136	390.236
Jun	386.062	387.708	389.477	386.266	386.874	388.269	387.442
Jul	384.334	384.237	383.772	383.944	383.311	390.921	385.086
Aug	380.840	382.624	377.427	385.281	379.127	387.203	382.083
Sep	384.597	385.960	383.519	386.977	383.908	388.064	385.504
Oct	382.696	380.381	381.705	386.212	382.923	386.792	382.451
Nov	380.102	380.392	379.268	378.431	378.226	381.053	380.745
Dec	367.913	372.392	374.693	372.434	367.971	371.596	372.500

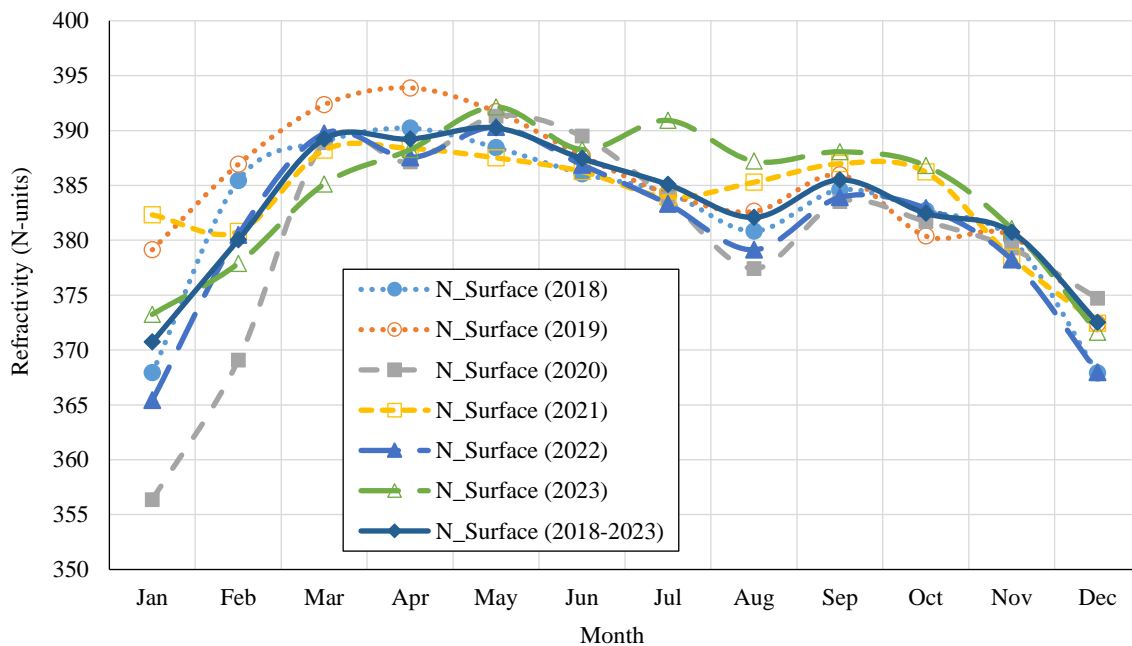


Figure 2. Monthly average variation of surface radio refractivity in Ikeja over the years 2018 to 2023.

This seasonal pattern of N_s (N-units) presented in Figure 2 shows that there exist two peaks of refractivity within a year, which then forms a letter “M” shape annually. The peaks are observed within the intense period of rainy/wet season of the coastal areas as reported in [11, 21, 22]. One peak occurs in May and the other in September, while the dip in August could be related to the well-known August-break phenomenon, where the amount of rain becomes reduced due to certain atmospheric conditions [22–24], thereby leading to a low refractivity.

The obtained average surface refractivity results for year 2018 display high N_s values occurring in the wet periods from March and September, peaking at $N_s = 390$ N-units in April. In 2019, high N_s values are also observed between March to September in the wet season, with a peak of $N_s = 394$ N-units in April. In 2020, high N_s values occur in similar months as in 2018 and 2019, observed in the wet season, with a peak of $N_s = 391$ N-units in May. For 2021, high N_s values are noted within the wet months of March to September, peaking at $N_s = 388$ N-units in April. The year 2022 also experiences high N_s values within the wet months as usual, with the highest value being at $N_s = 390$ N-units in May. Finally, in 2023, high N_s values occurred from April to September which are the typical wet months, peaking at $N_s = 392$ N-units in May. Consequently, the overall average for the years 2018–2023, exhibits the highest N_s value within the very wet months, leading to great effects of multipath fading.

There is a consistency in the pattern for all the years considered for the refractivity values and its overall average for all the years (2018–2023) shows that there are higher values of N_s in the middle of the year which signifies the wet seasonal periods. It can be observed that the periods indicating the worst months are around March to September where there exists considerable amount of rainfall in this coastal location within Nigeria.

Diurnal Variation of Surface Refractivity for a Period of Six Years Over a Coastal Location

The diurnal variation of surface refractivity over the coastal location under study across the entire period is illustrated in Figure 3. This plot displays the average hourly time mean from 0:00 to 23:00 local time at the surface level for both the dry and wet seasons of 2018–2023. The average hourly surface refractivity in the year 2018 ranges from 386 N-units to 389 N-units during the early hours (0:00–6:00 local time) and night hours (19:00–23:00 local time), decreasing to a minimum of about 376

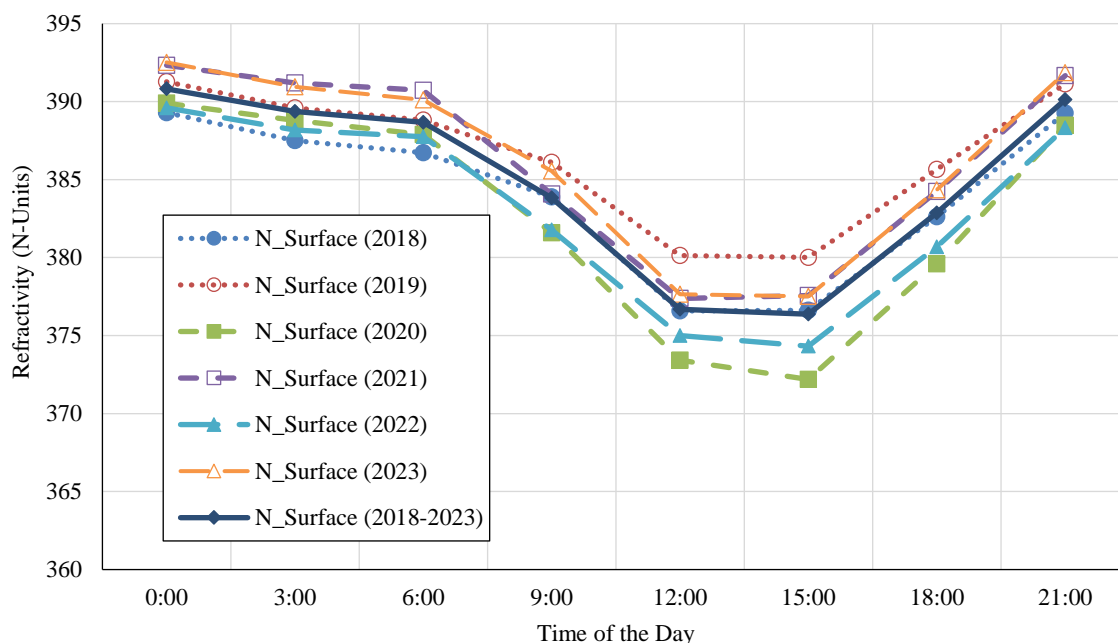


Figure 3. Diurnal average variation of surface radio refractivity over Ikeja for the years 2018 to 2023.

N-units around the afternoon hours (12:00–15:00 local time). In 2019, average surface refractivity is high, around 388 to 391 N-units, during the early and late hours, dropping at 6:00 local time to a minimum of 380 N-units around the afternoon hours (12:00–15:00 local time) local time. In 2020, mean surface refractivity is high between 387 and 390 N-units, during the early and late hours, dropping at 6:00 local time to a minimum of about 372 N-units around 15:00 local time. In 2021, average hourly surface refractivity ranges from 390 to 392 N-units during the early hours (0:00–6:00 local time) and late hours (19:00–23:00 local time), decreasing at 6:00 local time to a minimum of 377 N-units at both 12:00 and 15:00 local times. In 2022, average surface refractivity starts at 389 N-units in the early hours (0:00–6:00 local time), drops to a minimum of 374 N-units at 15:00 local time, and accordingly rises to a higher level of 388 N-units at 21:00 local time. In 2023, average surface refractivity is observed at high values of about 390 N-units to 393 N-units in the early hours to 6:00 local time, before dropping to a minimum of 377 N-units at 12:00 and 15:00 local times. In Ikeja, average surface refractivity across all the years (2018–2023) ranges from 388 to 390 N-units in the early hours, and then reducing to a minimum of 376 N-units at 15:00 local time.

In general, the diurnal variation pattern is consistent over all the years from 2018 to 2023, with high refractivity values in the early and late hours of the day and a drop starting around 06:00 local time, reaching a minimum around 15:00 local time before rising again towards the end of the day. This variation is linked to the earth’s response to solar insolation, the primary driver behind the observed weather conditions. These results align well with previous studies by Owolabi and Williams [25], indicating that diurnal surface refractivity in Nigeria is influenced by local meteorology.

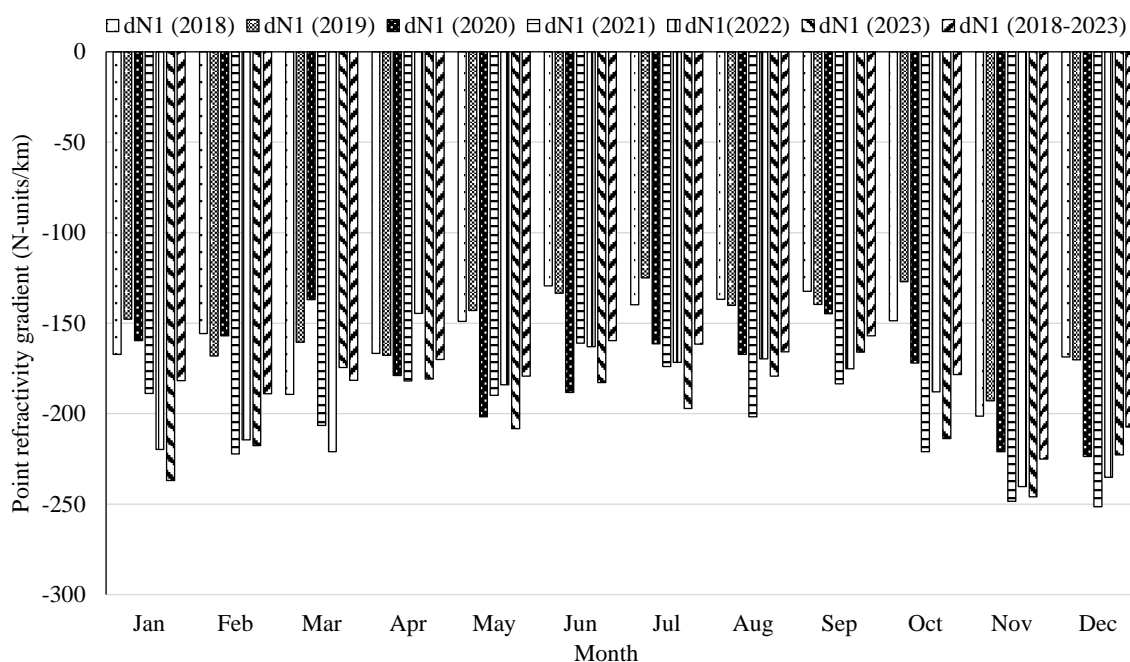
In summary, the diurnal variation of surface refractivity for the whole period under investigation (2018–2023) shows high values in the early morning and late night, with very low values between 12:00 and 15:00 local time for both dry and wet seasons.

Seasonal and Diurnal Variation of Point Refractivity Gradient

The computed seasonal data for the point refractivity gradient for Ikeja is shown in Table 3, which shows that across the six years, the refractivity gradient varied from -124 to -251 N-units/km. Figure 4 depicts the monthly variation of point refractivity gradient values at 70 m for the location under

Table 3. Point refractivity gradient at height of 70 m for different years.

Month	Point refractivity gradient, N-Units/km	Point refractivity gradient, N-Units/km	Point refractivity gradient, N-Units/km	Point refractivity gradient, N-Units/km	Point refractivity gradient, N-Units/km	Point refractivity gradient, N-Units/km
	2018	2019	2020	2021	2022	2023
Jan	-167.294	-147.688	-159.642	-188.737	-219.725	-236.952
Feb	-155.742	-168.125	-157.042	-222.250	-214.489	-217.611
Mar	-189.275	-160.549	-136.978	-206.516	-221.093	-174.493
Apr	-166.738	-167.688	-178.867	-181.993	-144.600	-180.900
May	-148.981	-143.020	-201.678	-189.842	-184.118	-208.249
Jun	-129.334	-133.420	-188.279	-161.114	-162.903	-182.819
Jul	-139.863	-124.974	-161.410	-173.951	-171.701	-197.167
Aug	-136.770	-140.229	-167.169	-201.760	-169.706	-179.259
Sep	-132.442	-139.606	-144.676	-183.435	-175.220	-165.975
Oct	-148.712	-126.999	-171.986	-221.024	-188.000	-213.854
Nov	-201.380	-192.928	-221.037	-248.389	-240.387	-245.953
Dec	-168.726	-170.240	-223.688	-251.396	-235.191	-222.822
Average	-157.105	-151.26	-176.037	-123.797	-285.430	-310.536

**Figure 4.** Monthly point refractivity gradient estimation for Ikeja over the years 2018 to 2023.

study over the years 2018 to 2023. It was observed during the whole period under study that the monthly average point refractivity values (dN_1) are higher in the peak of rainy period (April to September) than in the dry-season months (especially November to February).

The months of March and October, which often signify the starting and closing of the rainy periods, both show lower refractivity gradients compared to the period of intense rain. All through the dry months, the dN_1 values fluctuate from -148 to -201 , -126 to -192 , -157 to -223 , -188 to -251 , -188 to -240 and -213 to -245 N-units/km for the years 2018, 2019, 2020, 2021, 2022, and 2023,

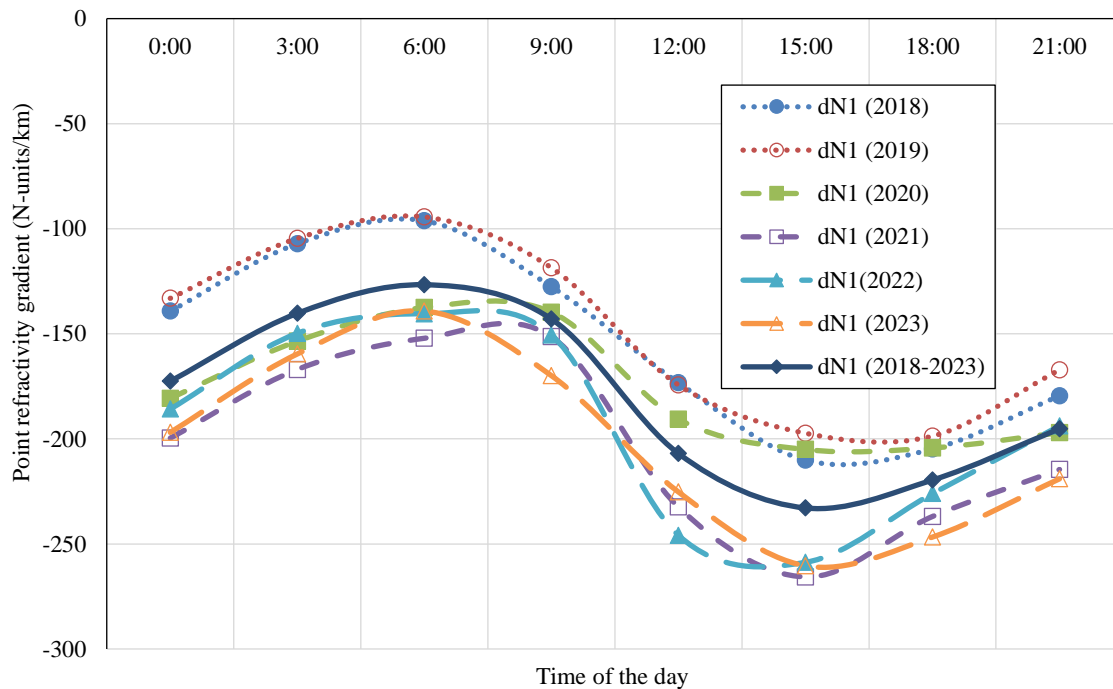


Figure 5. Diurnal variation of point refractivity gradient for Ikeja over the years 2018 to 2023.

respectively. Whereas, throughout the wet season, it oscillates from -129 to -189 , -124 to -167 , -136 to -201 , -161 to -206 , -144 to -221 and -165 to -208 N-units/km for the years 2018, 2019, 2020, 2021, 2022, and 2023, respectively. Also, the range of dN_1 values for the entire period is from -178 to -225 and -156 to -181 N-units/km for the dry and wet seasons, respectively, and the overall mean for individual seasons are -196.30 N-units/km -167.83 N-units/km, respectively. Thus, the worst months take place in the rainy season, specifically between April and September, across the various years investigated. As such, this is credited to the high amount of the atmosphere's water vapor content in this period.

Figure 5 shows the diurnal distribution of the point refractivity gradient across all the years from 2018 to 2023 for the coastal location under study. It was observed from this result that the diurnal analysis performed for dN_1 N-units/km follows the same trend across all the years. The dN_1 values were observed to be lower during the afternoon hours between 12:00 and 18:00 local time, with the lowest values occurring around 15:00 local time across all the years. For the cumulative years (2018-2023), the overall lowest value (-232.90 N-units/km) occurred at 15:00 local time and overall highest value (-126.65 N-units/km) occurred at 06:00 local time.

Seasonal Variation of Geoclimatic Factor

When designing terrestrial line-of-sight systems, it is essential to incorporate a fade margin that accounts for multipath fading into the link budget. The ITU-R recommended that multipath fading typically considers many factors such as the path distance, operating frequency, path inclination, and the geoclimatic factor of the specific region [14]. As demonstrated by Odedina and Afullo [3] and Etokebe et al. [11], the fade margin is directly proportional to the geoclimatic factor. The ITU-R suggests that the K value, determined from regional data, accurately predicts multipath fading.

Therefore, one of the critical elements in determining the multipath fade margin is the K value during the worst month, corresponding to the month with the highest K value. Table 4 displays the monthly mean geoclimatic factor values for Ikeja.

Table 4. Monthly average geoclimatic factor (K) for different years.

Month	Geoclimatic factor (K)	Geoclimatic factor (K)	Geoclimatic factor (K)	Geoclimatic factor (K)	Geoclimatic factor (K)	Geoclimatic factor (K)
	2018	2019	2020	2021	2022	2023
Jan	0.0001552	0.0000669	0.00020530	0.0009797	0.0001801	0.0001381
Feb	0.0000775	0.0000969	0.00012394	0.0001333	0.0001189	0.0001603
Mar	0.0001179	0.0000950	0.00078215	0.0001095	0.0001197	0.0009961
Apr	0.0000891	0.0000994	0.00890732	0.0009540	0.0007862	0.0009304
May	0.0000802	0.0000752	0.00010781	0.0009538	0.0009561	0.0001115
Jun	0.0000649	0.0000654	0.00010278	0.0008674	0.0008587	0.0009028
Jul	0.0000669	0.0000601	0.00078785	0.0008556	0.0008282	0.0001006
Aug	0.0000671	0.0000641	0.00079537	0.0009951	0.0008371	0.0008924
Sep	0.0000660	0.0000680	0.00070572	0.0009376	0.0008515	0.0007990
Oct	0.0000763	0.0000631	0.00088805	0.0001531	0.0009811	0.0001224
Nov	0.0001172	0.0001227	0.0001259	0.0001796	0.0001667	0.0002243
Dec	0.0000888	0.0001253	0.0001370	0.00015279	0.0001527	0.0001641
Average	0.0000889	0.0000835	0.0004715	0.00060595	0.0005697	0.0004618

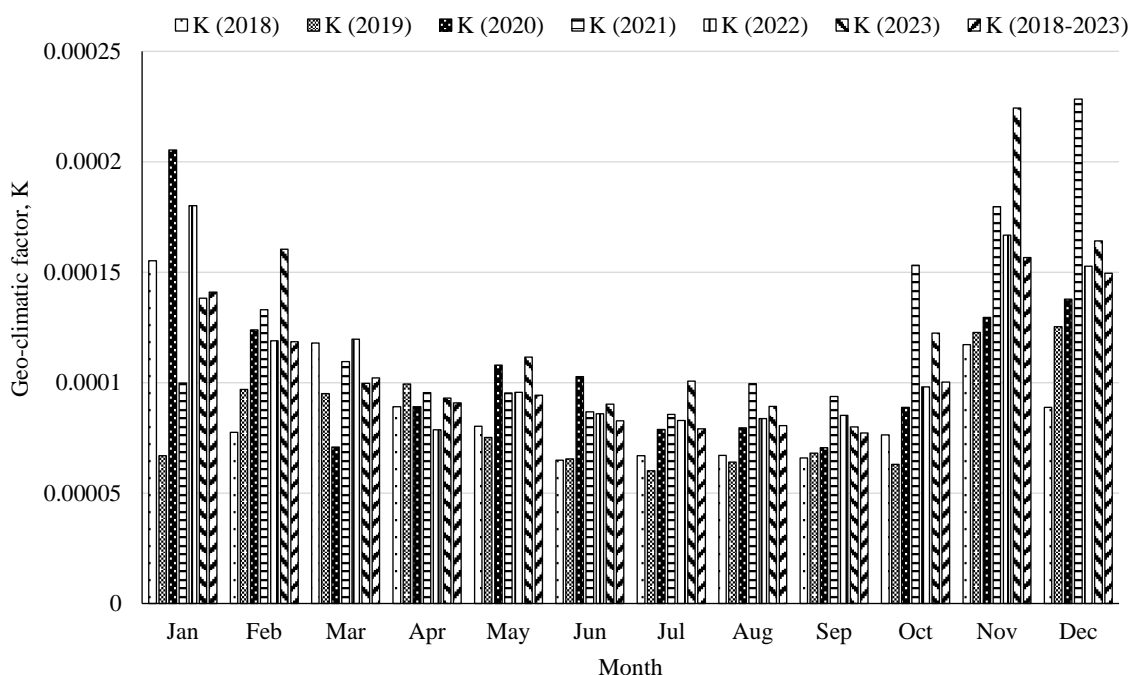
**Figure 6.** Monthly variation of geoclimatic factor for Ikeja over the years 2018 to 2023.

Figure 6 shows the plots of the monthly variation of the geoclimatic factor for the study location over the years 2018 to 2023. For the year 2018, high K values occur in January, March, and November, peaking at $K = 0.00016$ in January. In 2019, high K values are observed in November and December, with a peak of $K = 0.00013$ in December. In 2020, high K values occur in January, February, November, and December, with a peak of $K = 0.00021$ in January. For 2021, high K values are noted in February and from October to December, peaking at $K = 0.00023$ in December. The year 2022 experiences high K values in January, November, and December, with the highest value being $K = 0.00018$ in January. Finally, in 2023, high K values occurred in January, February, November, and December, which are the typical dry months, peaking at $K = 0.00022$ in November. Consequently, the overall average exhibits

the highest K values within the very dry months in the city studied. There is a consistency in the pattern for all the years considered for the geoclimatic factor and its overall average for all the years (2018–2023) shows that there is a drop in K in the middle of the year, which signifies the wet seasonal periods. It can be observed that the periods indicating the worst months are around June to September where there exists the peak of the rainy season in this tropical location within Nigeria.

Diurnal Variation of Geoclimatic Factor

Figure 7 shows the diurnal variation of the geoclimatic factor (K) across all the years from 2018 to 2023 for the coastal location under study. Similar patterns of the average diurnal evaluation of K were observed for all the individual years considered, such that the overall lowest was at the early morning hours (around 06:00 local time) and the highest occurred during the peak of the afternoon (between 15:00 and 18:00 local time). The results indicates that $K = 6.49E - 05$ occurred at 06:00 local time and $K = 0.00016$ occurred at 18:00 local time are the lowest and the highest average K values, respectively, for the joint years (2018–2023).

Seasonal Variation of Refractivity Gradient and Geoclimatic Factor over a Coastal Location

From the results presented in Tables 5 and 6, it can be observed that there are seasonal based variations in the dN_1 and K values across all the years studied for Ikeja. These disparities have been shown in Figures 8 and 9. The identification numbers (ID) given in the tables suggests the wet and dry months plotted in Figures 8 and 9. Figure 8 shows that the wet season mean dN_1 is observed to be -167.828 N-units/km, while the dry season average dN_1 is given as -196.296 N-units/km. As a result of this, it can be said that dN_1 is higher during the rainy periods compared to the dry months.

On the contrary, the average values of the geoclimatic factor presented in Figure 9 show that the wet season is $8.66774E - 05$ and that of the dry season is 0.000133 . Thus, the value of K is higher in the dry season than in the wet season.

The high variability of refractivity gradient experienced in the wet season (as shown in Figure 8) can be ascribed to the increase in the water vapor amount in the atmosphere in the observed period.

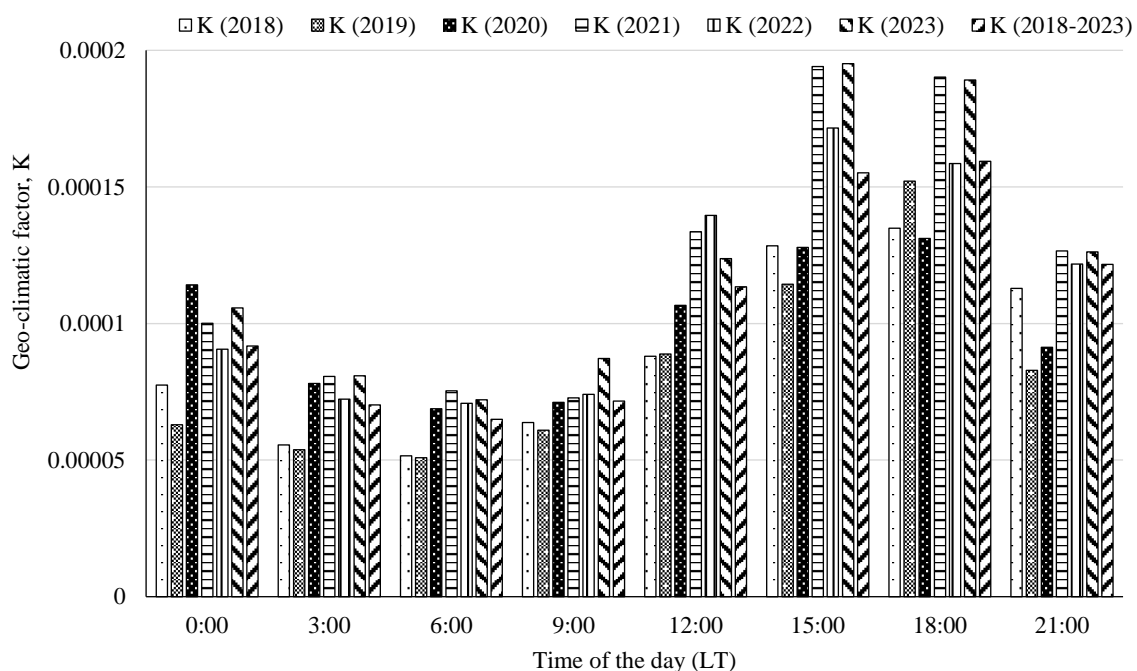


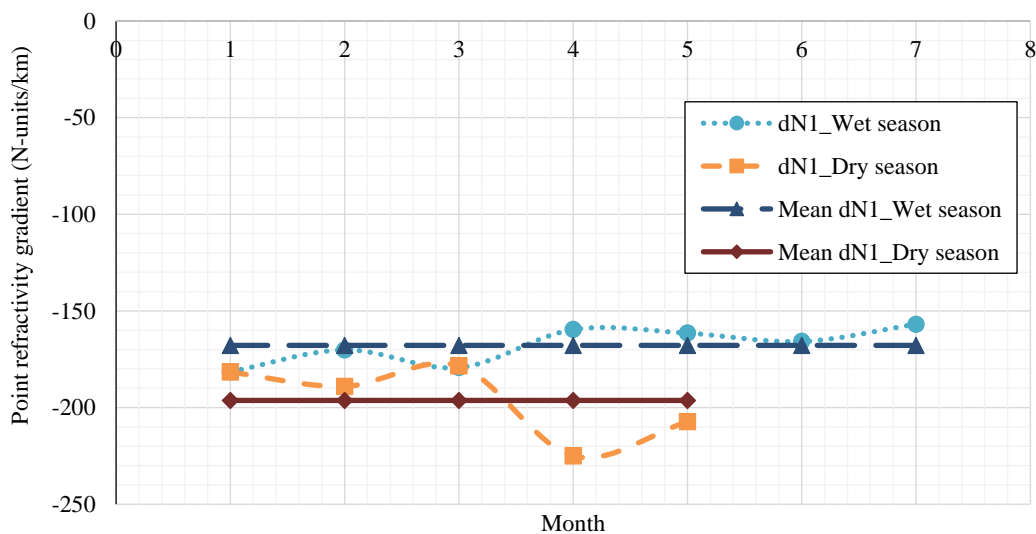
Figure 7. Diurnal variation of geoclimatic factor for Ikeja over the years 2018 to 2023.

Table 5. Average point refractivity gradient for the wet and dry season months in Ikeja.

ID	Month (wet season)	dN_1 (N-units/km) for wet season months (2018–2023)	Month (dry season)	dN_1 (N-units/km) for dry season months (2018–2023)
1	Mar	-181.485	Jan	-181.673
2	Apr	-170.132	Feb	-189.020
3	May	-179.315	Oct	-178.429
4	Jun	-159.645	Nov	-225.013
5	Jul	-161.512	Dec	-207.344
6	Aug	-165.816		
7	Sep	-156.893		
	Average dN_1 for wet-season months	-167.8280807	Average dN_1 for dry-season months	-196.296

Table 6. Average geoclimatic factor for the wet and dry season months in Ikeja.

ID	Month (wet season)	K for wet-season months (2018–2023)	Month (dry season)	K for dry-season months (2018–2023)
1	Mar	0.000102094	Jan	0.000140914
2	Apr	9.07843E-05	Feb	0.000118474
3	May	9.43056E-05	Oct	0.000100326
4	Jun	8.26694E-05	Nov	0.000156671
5	Jul	7.9135E-05	Dec	0.00014953
6	Aug	8.05207E-05		
7	Sep	7.72325E-05		
	Average K for wet-season months	8.66774E-05	Average K for dry-season months	0.000133183

**Figure 8.** Seasonal variation of point refractivity gradient (dN_1) for the wet and dry season months over the years 2018 to 2023.

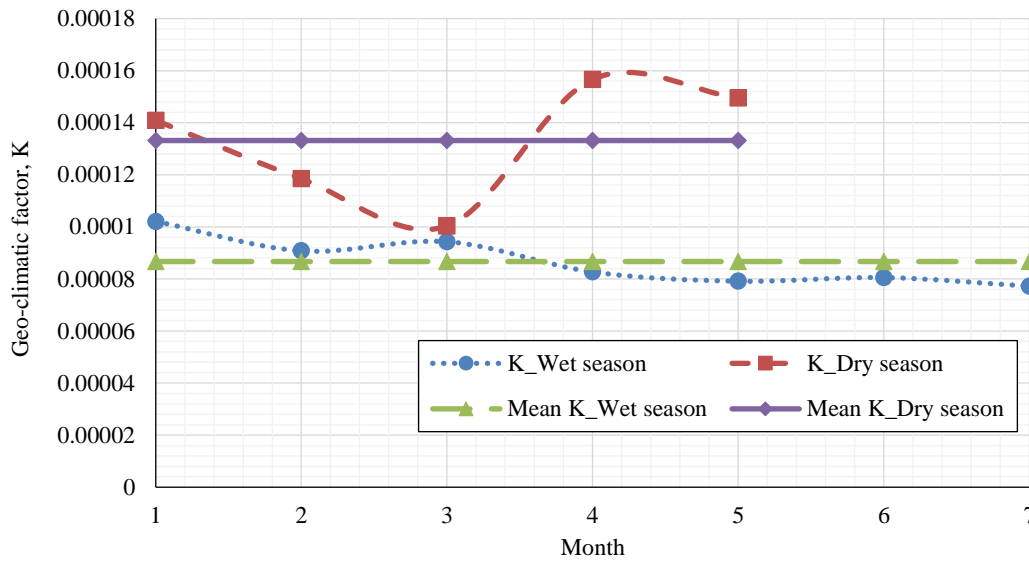


Figure 9. Seasonal variation of geoclimatic factor (K) for the wet and dry season months over the years 2018 to 2023.

Long-Term Cumulative Distribution of Refractivity Gradient

The CDF of the refractivity gradient is required in evaluating anomalous propagation state of radio signals. The long-term CDF for Ikeja over the years 2018–2023 presented in Figure 10 shows the classification of the refractive gradient values into different refractive conditions (as shown in Table 1). During the entire period, the range of dN_1 oscillates between -993 and 964 N-units/km, and the values of dN_1 converge around 100 N-units/km. Across the six-year data, the likelihood of the existence of sub-refraction, super-refraction, and ducting conditions ranges between $15\% - 42\%$, $5\% - 30\%$, and $45\% - 75\%$, respectively.

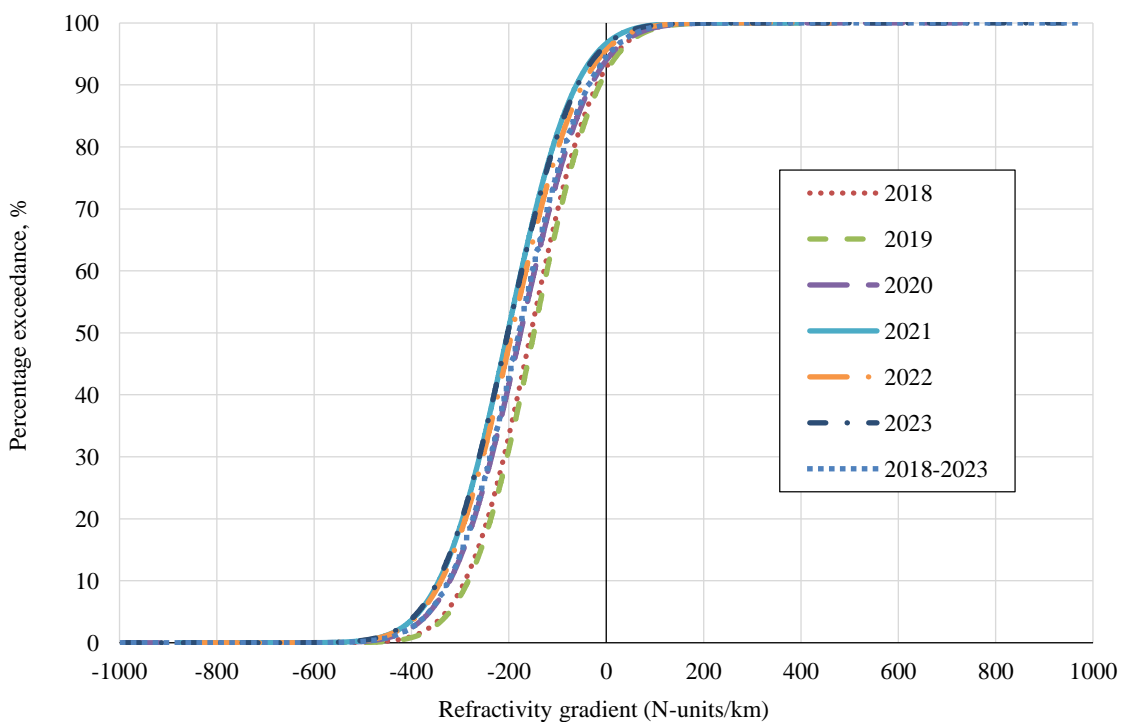


Figure 10. Long-term cumulative distribution of refractivity gradient over Ikeja.

CONCLUSION

Using six years' data of the ECMWF database, the point refractivity gradient and geoclimatic factor necessary for radio communication links design have been computed for Ikeja, a coastal location in Nigeria. The results obtained vividly indicate that the refractivity gradient and geoclimatic values varies seasonally and diurnally across Ikeja. In the wet months, high variability of refractivity gradient ($dN_1 = -167.828$ N-units/km) was experienced which can be attributed to the increase in the water vapor amount in the atmosphere in that period, compared to the dry periods with low variability of about $dN_1 = -196.296$ N-units/km. Also, the average values of the geoclimatic factor show that its value in the wet season is $8.66774E - 05$ and that of the dry season is 0.000133 . The value of K is higher in the dry season than in the wet season. Thus, this suggests that extremely poor radio propagation condition is expected to take place within the dry months especially in November as a result of extreme values of both dN_1 and K , unlike in September that has lowest dN_1 and K values. Hence, the parameters derived in this work are recommended for radio link budget calculations in the planning and designing of terrestrial microwave links.

REFERENCES

1. Bettouche Y, Agba BL, Kouki AB. Geoclimatic factor and point refractivity evaluation in Quebec-Canada. 2014 XXXIth General Assembly and Scientific Symposium (URSI GASS), Beijing, China, August 16–23, 2014. pp. 1–4.
2. Dinc E, Akan O. Beyond-line-of-sight communications with ducting layer. *IEEE Commun Mag.* 2014; 52 (10): 37–43.
3. Odedina PK, Afullo TJO. Use of spatial interpolation technique for the determination of the geoclimatic factor and fade depth calculation for Southern Africa. *Proceedings of IEEE AFRICON 2007*, Windhoek, South Africa, September 26–28, 2007. pp. 1–7.
4. Olsen RL, Segal B. New techniques for predicting the multipath fading distribution on VHF/UHF/SHF terrestrial line-of-sight links in Canada. *Can J Electric Computer Eng.* 1992; 17 (1): 11–23.
5. Olsen RL, Tjelta T. Worldwide techniques for predicting the multipath fading distribution on terrestrial L.O.S. links: background and results of tests. *IEE Trans Antennas Propagation.* 1999; 47 (1): 157–170.
6. Adediji AT, Mandeep JS, Ismail M. Meteorological characterization of effective earth radius factor (k-factor) for wireless radio link over Akure, Nigeria. *MAPAN – J Metrol Soc India.* 2014; 29: 131–141. doi: 10.1007/s12647-013-0074-9.
7. Karimian AC, Yardim, C, Hodgkiss WS, Gerstoft P, Barrios AE. Estimation of radio refractivity using a multiple angle clutter model. *Radio Sci.* 2012; 47 (3): RS0M07. doi: 10.1029/2011RS004701.
8. Ojo OL, Ajewole MO, Ojo JS. Estimation of clear-air fades depth due to radio climatological parameters for microwave link applications in Akure, Nigeria. *Int J Eng Appl Sci.* 2015; 7 (3): 8269.
9. Asiyo MO, Afullo TJO. Statistical estimation of fade depth and outage probability due to multipath propagation in Southern Africa. *Prog Electromagn Res B* 2013; 46: 251–274.
10. Tjelta T, Olsen RL, Martin AL. Systematic development of new multivariable techniques for predicting the distribution of multipath fading on terrestrial microwave link. *IEEE Trans Antennas Propagation.* 1990; 38: 1650–1665.
11. Etokebe IJ, Uko MC, Chinwe IU. Determination of refractivity gradient and geoclimatic factor using radiosonde data and inverse distance weighting spatial interpolation for missing data. *Int J Syst Sci Appl Math.* 2016; 1 (4): 76–81. doi: 10.11648/j.ijssam.20160104.17.
12. Oluwafemi IB, Olla MO. Estimation of geoclimatic factor for Nigeria through meteorological data. *Eur J Electric Eng Computer Sci.* 2021; 5 (3): 41–44. doi: 10.24018/ejece.2021.5.3.191.
13. Grabner M, Kvicera V. Introduction to project of refractive index measurement in Prague. Twelfth International Conference on Antennas and Propagation, 2003 (ICAP 2003) (Conf. Publ. No. 491), Exeter, UK, March 31–April 3, 2003. Vol. 2, pp. 784–787.

14. ITU-R. Propagation Data and Prediction Methods Required for the Design of Terrestrial Line-of-Sight Systems. Recommendation of ITU-R P.530-14. Geneva, Switzerland: ITU-R; 2012.
15. Serdega V, Ivanovs G. Refraction seasonal variation and that influence on to GHz range microwaves availability. *Elektronika ir Elektrotechnika*. 2015; 78 (6): 39–42.
16. IUT-Radio Communication Assembly. Propagation Data and Prediction Methods Required for the Design of Terrestrial Line-of-Sight Systems. IUT-R P.530-16. Geneva, Switzerland: ITU-R; 2015.
17. ITU-R Rec 834-4: Effects of Tropospheric Refraction on Radiowave Propagation. Geneva, Switzerland: International Telecommunication Union, ITU; 2003.
18. Afullo TJ, Adongo MO, Motsoela T, Molotsi DF. Refractivity gradient and k-factor in Botswana. In: Proceedings of the Third Regional Workshop on Radio Communications in Africa: Radio Africa '99. Trans SA Inst Electric Eng. 2001: 107–110.
19. Bean BR, Dutton EJ. Radio Meteorology. National Bureau of Standard Monographs. Washington, DC, USA: US Department of Commerce; 1996. 132pp.
20. Akpootu DO, Iliyasu MI. Estimation of tropospheric radio refractivity and its variation with meteorological parameters over Ikeja, Nigeria. *J Geogr Environ Earth Sci Int*. 2017; 10 (1): 1–12.
21. Ezeh CU, Obeta MC, Raymond NC. Variations in the sequences of daily rainfall across Nigeria. *Arab J Geosci*. 2016; 9: 681. doi: 10.1007/s12517-016-2719-9.
22. Adedeji T, Utah EU, Sombos TE. Monthly variation and annual trends of rainfall across major climatic zones in Nigeria. *IOSR J Appl Phys*. 2018; 10 (4): 15–28.
23. Olaniran OJ, Sumner GN. A study of climatic variability in Nigeria based on the onset, retreat, and length of the rainy season. *Int J Climatol*. 1989; 9: 253–269.
24. Lawal YB, Falodun SE, Ojo JS. Temporal evolution of atmospheric parameter-profiling on rain height over two geoclimatic regions in Nigeria. *J Atmos Solar Terres Phys* 2020; 211: 105482. doi: 10.1016/j.jastp.2020.105482.
25. Owolabi IE, Williams VA. Surface radio refractivity patterns in Nigeria and the Southern Cameroon. *J West Afr Sci Assoc*. 1970; 1: 3–17.